STRUCTURES AND MECHANISM OF HEAT AND MASS TRANSPORT PHENOMENA IN TURBULENT BOUNDARY LAYER WITH SEPARATION AND REATTACHMENT

Hirofumi Hattori, Tomoki Noda, Masato Tagawa
Department of Mechanical Engineering
Nagoya Institute of Technology
Gokiso-cho, Showa-ku, Nagoya 466-8555, JAPAN
hattori@nitech.ac.jp

Yasutaka Nagano
Nagoya Industrial Science Research Institute
Nagoya Institute of Technology
naganoy2@asme.org

ABSTRACT

This paper presents observations and investigations of the detailed structure and mechanism of turbulent heat and mass transfer in turbulent boundary layer with separation and reattachment by means of direct numerical simulation. In order to observe turbulent heat and mass transfer in a boundary layer with reattachment and separation, DNSs of boundary layer with heat and mass transfer over a forward-facing step or a 2-dimensional block are carried out. The present DNSs demonstrate near-wall distributions of statistics of turbulent quantities which relate to heat and mass transfer around separation and reattachment points. Also, instantaneous turbulent heat and mass transfer are indicated so as to investigate a relation between instants and statistics of turbulent quantities, which can show heat and mass transfer mechanism in turbulent boundary layer with separation and reattachment. The quadrant analysis is carried out to investigate the turbulence motion for the production of Reynolds shear stress and wall-normal turbulent heat flux, in which it is revealed that $Q1$ and $Q3$ events (i.e., interactions) affect these quantities on the 2-D block.

INTRODUCTION

The objectives of this study are to investigate and discuss structures and mechanism of transport phenomena in turbulent boundary layers with separation and reattachment in detail, and to reconstruct and assess turbulence models in LES and RANS for predictions of transport phenomena in complex turbulent flows. The phenomena of flow separation and reattachment often occur in various flow situations. Especially, a strong pressure gradient of mean flow of boundary layer and a complex shape of wall cause the flow separation and reattachment, which also induce the dissimilarity between velocity and thermal fields. Considering an enhancement of heat and mass transfer, the flow separation and reattachment affect heat and mass transfer for the better, but those yield an increase in friction and pressure drop of flow. Thus, simultaneous controls of flow, heat and mass transfer are very difficult issue for the engineering. Moreover, in such flows, it is difficult to predict and measure distributions of turbulence, heat and mass, since various types of machinery, building structures and terrain complicate transport phenomena of the kind. On the other hand, direct numerical simulation (DNS) is a very useful technique in order to determine such detailed turbulet transport phenomena as well as experimental techniques. Especially, near-wall structure and mechanism of turbulent heat and mass transfer can be clarified by DNS. The authors have been conducting DNSs of a boundary layers, and flow databases have been constructed, in which the turbulent characteristic of the thermally stratified boundary layer (Hattori *et al.*, 2007) and the boundary layer over forward-facing step are investigated (Hattori and Nagano, 2010) in detail. Also, the prediction performances of turbulence models have been evaluated using DNS in order to improve the turbulence model for prediction of turbulent flows (e.g., Hattori *et al.* (2009)). However, we need to reveal the more complex flow, heat and mass transfer phenomena involving turbulence of the physical interest, and improve the turbulence model of LES, RANS and the hybrid LES/RANS for the engineering.

In the present study, in order to investigate and discuss structures and mechanism of transport phenomena in turbulent boundary layer with separation and reattachment in more detail, DNSs of the turbulent heat and mass transfer in boundary layer over an obstacle which strongly causes a flow separation and reattachment are performed. A forward-facing step and a 2-dimensional block are selected for the shapes of obstacle in the present study, in which the height and the width of step or 2-D block and Reynolds number defined by the momentum thickness of inlet boundary layer are varied so as to investigate influences of obstacle to the phenomena of heat and mass transfer subject to flow separation and reattachment.

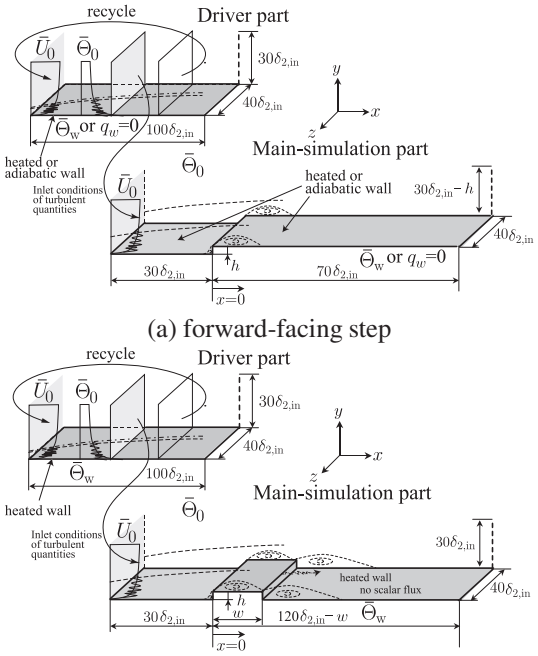

(a) forward-facing step

(b) 2-dimensional block

Figure 1. Computational domains and coordinate systems

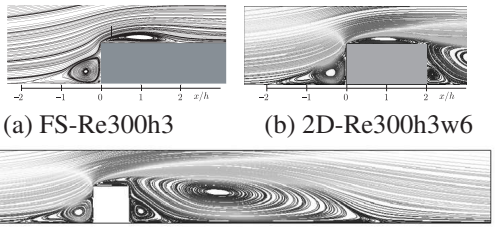

(a) FS-Re300h3 (b) 2D-Re300h3w6

(c) 2D-Re300h3w3

Figure 2. Streamlines around step or block

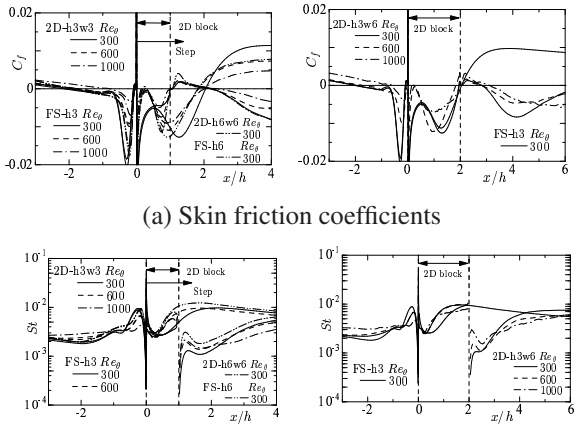

(a) Skin friction coefficients

(b) Stanton numbers

Figure 3. Distributions of skin friction coefficients and Stanton numbers around step or block

DNS OF BOUNDARY LAYER WITH SEPARATION AND REATTACHMENT

The governing equations used in DNS are the Navier-Stokes equation without buoyancy, the continuity equation for the velocity field, and the energy equation for the thermal field, in which incompressibility is assumed as follows:

$$\frac{\partial u_i^*}{\partial x_i^*} = 0 \tag{1}$$

$$\frac{\partial u_i^*}{\partial t^*} + u_j^* \frac{\partial u_i^*}{\partial x_j^*} = -\frac{\partial p^*}{\partial x_i^*} + \frac{1}{Re_{\delta_{2,\mathrm{in}}}} \frac{\partial^2 u_i^*}{\partial x_j^* \partial x_j^*} \tag{2}$$

$$\frac{\partial \theta^*}{\partial t^*} + u_j^* \frac{\partial \theta^*}{\partial x_j^*} = \frac{1}{Re_{\delta_{2,\mathrm{in}}} Pr} \frac{\partial^2 \theta^*}{\partial x_j^* \partial x_j^*} \tag{3}$$

where the Einstein summation convention applies to repeated indices, and a comma followed by an index indicates differentiation with respect to the indexed spatial coordinate. u_i^* is the dimensionless velocity component in x_i direction, p^* is the dimensionless pressure, t^* is the dimensionless time, and x_i^* is the dimensionless spatial coordinate in the i direction, respectively. All equations are non-dimensionalized by the free stream velocity, $\bar{U}_0$, and the momentum thickness, $\delta_{2,\mathrm{in}}$, at the inlet of the driver part which generates turbulence for the inlet boundary condition of main simulation part indicated as in Fig. 1. Here, Fig. 1 also shows computational domains, schematics and the coordinate systems of the present DNSs, in which the boundary layers with heat and mass transfer over the forward-facing step or the 2-dimensional block as the typical separated and attached flow are illustrated. The present DNS based on the high-accuracy finite-difference method (Hattori *et al.*, 2007; Hattori and Nagano, 2010) is carried out under conditions of Reynolds numbers based on the free stream velocity and the momentum thickness at the inlet of the driver part, $Re_{\delta_{2,\mathrm{in}}}$=300, 600 and 1000, in order to explore the influence of the Reynolds number in the present condition. The height of step or 2-D block, h, is fundamentally set to $3\delta_{2,\mathrm{in}}$, but is also set to $6\delta_{2,\mathrm{in}}$ in the case of $Re_{\delta_{2,\mathrm{in}}}$=300 in order to observe the effect of the step height on turbulence. These heights are about $1/3 \sim 2/3$ of the boundary layer thickness at the inlet of the driver. In the DNS of 2-D block, the width of 2-D block is set to $3\delta_{2,\mathrm{in}}$, $6\delta_{2,\mathrm{in}}$ and $9\delta_{2,\mathrm{in}}$.

The boundary conditions for the velocity field are the non-slip conditions on the walls, and $\partial u/\partial y = 0$, $\partial w/\partial y = 0$, $\partial v/\partial y = -(\partial u/\partial x + \partial w/\partial z)$ on the upper boundary (free stream). At the outlet of both parts, convective boundary conditions are applied, and periodic boundary conditions are used in the spanwise direction. The uniform temperature wall condition is configured for the thermal field of both the forward step and the 2-D block cases. The grid numbers is $x \times y \times z = 384 \times 128 \times 128$.

RESULTS AND DISCUSSIONS

Turbulent heat and mass transfer around obstacles

Figure 2 shows the typical patterns of streamline around the step or the block in boundary layers. It can be seen

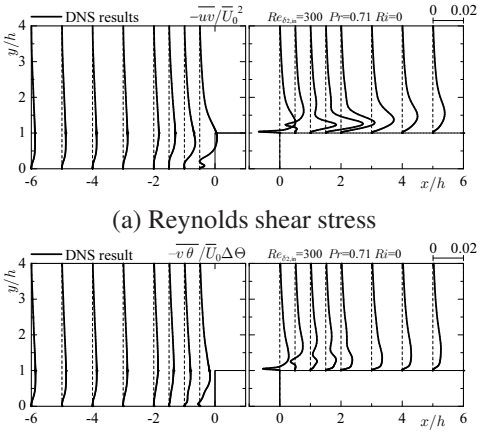

Figure 4. Distributions of turbulent quantities in forward-facing step flow (FS-Re300h3)

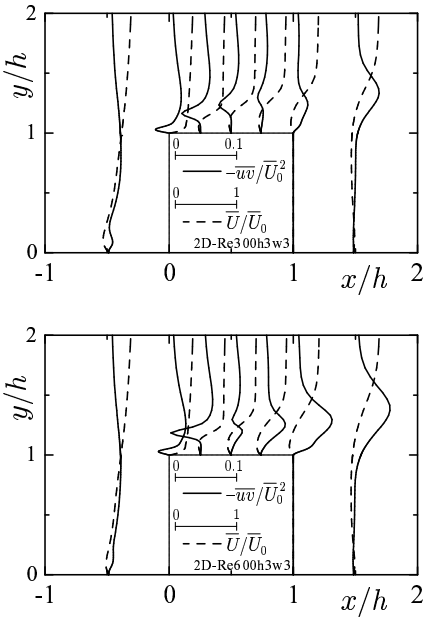

Figure 5. Profiles of streamwise mean velocity and Reynolds shear stress around 2D-block

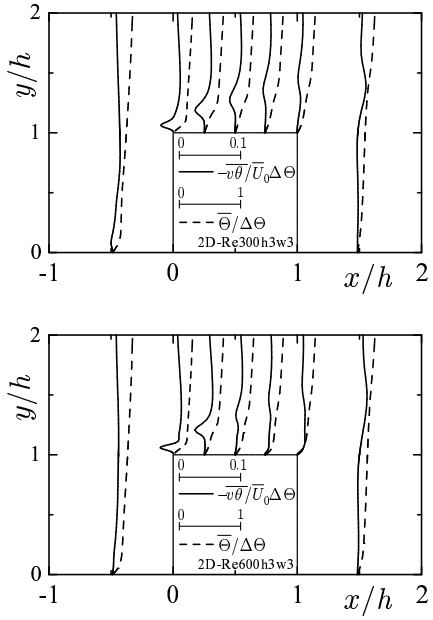

Figure 6. Profiles of mean temperature and wall-normal turbulent heat flux around 2D-block

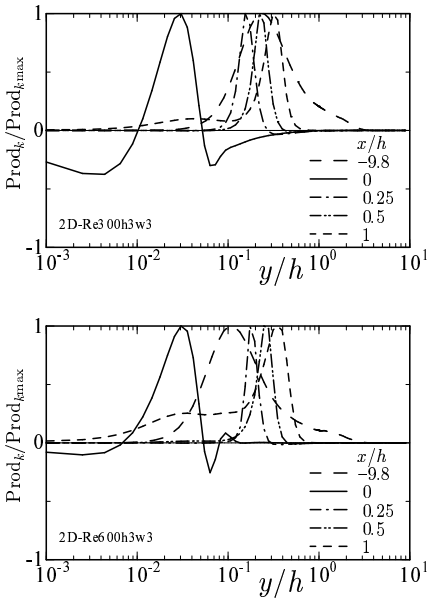

Figure 7. Production term in transport equation of k

that the flow separations and reattachments are clearly formed the around step or the block. Note that the reference "FS-Re300h3" means the case of forward step, Reynolds number, $Re_{\delta_2} = 300$, and the step height, $h = 3\delta_2$. Also, the reference "2D-Re300h3w6" means the case of 2-D block, Reynolds number, $Re_{\delta_2} = 300$, the step height, $h = 3\delta_2$, and the step width, $w = 6\delta_2$. In Fig. 2(c), the case of 2D-Re300h3w3 obviously shows a recirculation region and a secondary flow region behind the block, but the reattachment on the block is not observed in this case, though the reattachment on the block appears in the case of 2D-Re300h3w6 as shown in Fig. 2 (b).

The distributions of friction coefficient, C_f, and Stanton number, St, around the step or the block are indicated in Fig. 3. The dissimilarity between velocity and thermal field is obviously found by observing these figures. The distributions of C_f in the cases of 2-D block indicate similar trend with these of the cases of forward step to the vicinity of the center of the block. In the lowest Reynolds number of both the cases, C_f remarkably decreases near the front corner of step or block. This is because that the negative value of Reynolds shear stress often appears around here as shown in Figs. 4 and 5, although the gradient of streamwise mean velocity indicates the positive value. This might be the counter gradient diffusion phenomenon (CDP) Hattori and Nagano (2010), which of

Table 1. Reattachment and maximum Stanton number points behind 2-D block

$Re_{\delta_{2,\mathrm{in}}}$	Reattatchment points: $X_r[(x-w)/h]$/ Maximum Stanton number points:$X_{str}[(x-w)/h]$			
300	2D-Re300h3w3	2D-Re300h3w6	2D-Re300h3w9	2D-Re300h6w6
	7.40/ 5.85	4.51/ 4.64	4.25/ 3.85	8.74/ 6.88
600	2D-Re600h3w3	2D-Re600h3w6	——	——
	7.89/7.64	5.07/ 4.43	———	———
1000	2D-Re1000h3w3	2D-Re1000h3w6	——	——
	9.5/ 7.13	5.79/ 4.96	———	———

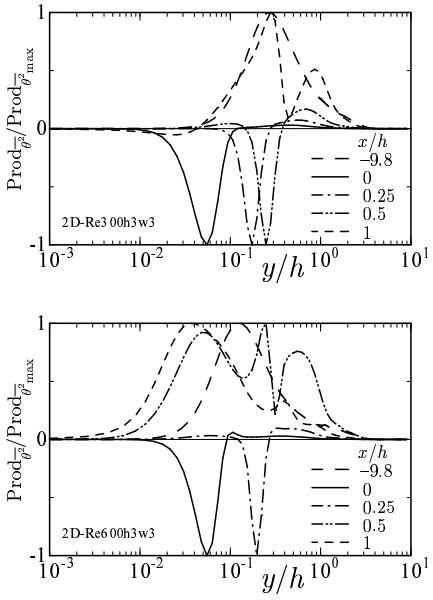

Figure 8. Production term in transport equation of $\overline{\theta^2}$

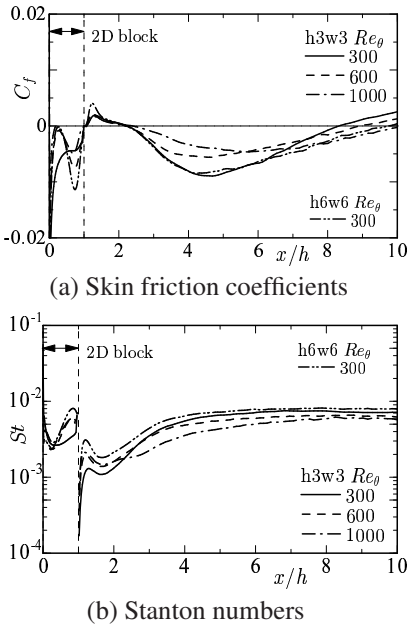

(a) Skin friction coefficients

(b) Stanton numbers

Figure 9. Distributions of C_f and St behind 2-D block (2D-Re300h3w3)

turbulence is defined by the relation between the mean velocity gradients and Reynolds shear stress. In the thermal field, Stanton number also decreases near the front corner of step or block in all cases. On the other hand, the negative value of wall-normal turbulent heat flux is often observed near the front corner as shown in Figs. 4 and 6. Since the mean temperature gradient takes absolutely the positive value, this distribution indicates the CDP of turbulent heat transfer. Thus, Stanton number decreases due to CDP.

Next, in order to explain more the effect of CDP of turbulent heat and mass transfer, the quantity multiplying the mean velocity gradients by Reynolds shear stress is shown in Fig. 7, which clearly means the production of turbulence energy, where the production of turbulence energy, $P_k = -\overline{u_i u_j}(\partial \bar{U}_i/\partial x_j) = -\overline{uv}(\partial \bar{U}/\partial y + \partial \bar{V}/\partial x) - \overline{u^2}(\partial \bar{U}/\partial x) - \overline{v^2}(\partial \bar{V}/\partial y)$, indicates the positive sign in general. However, the production obviously indicates the negative sign near the front corner of step or block as shown in Fig. 7, because the Reynolds shear stress is the negative sign, even if the mean velocity gradient is the positive sign. Thus, it can be observed that the CDP of turbulence occurs. Since the CDP disturbs the turbulence transport, C_f decreases near the front corner of step or block at the case of the lowest Reynolds number. Note that using the linear gradient diffusion model of Reynolds stress as $-\overline{u_i u_j} = \nu_t(\partial \bar{U}_i/\partial x_j + \partial \bar{U}_j/\partial x_i) - (2/3)\delta_{ij}k$ where ν_t is the eddy diffusivity for momentum, P_k can be represented as $P_k = \nu_t(\partial \bar{U}/\partial y + \partial \bar{V}/\partial x)^2 + 2\nu_t[(\partial \bar{U}/\partial x)^2 + (\partial \bar{V}/\partial x)^2]$ in this situation. Thus, the negative value of P_k means the negative value of ν_t, and the CDP of velocity field can be defined by the negative value of ν_t.

As for the thermal field, the similar phenomenon is also found in the production of temperature variance, $P_{\overline{\theta^2}} = -2\overline{u_j\theta}(\partial \bar{\Theta}/\partial x_j) = -2\overline{u\theta}(\partial \bar{\Theta}/\partial x) - 2\overline{v\theta}(\partial \bar{\Theta}/\partial y)$ as shown in Fig. 8, but it can be observed that the negative value of $P_{\overline{\theta^2}}$ often occurs as compared with P_k. $P_{\overline{\theta^2}}$ can be represented as $P_{\overline{\theta^2}} = 2\alpha_t[(\partial \bar{\Theta}/\partial x)^2 + (\partial \bar{\Theta}/\partial y)^2]$ using the concept of eddy diffusivity for heat, α_t, as $\overline{u_j\theta} = -\alpha_t(\partial \bar{\Theta}/\partial x_j)$. Thus, the CDP of thermal field means the negative value of α_t.

Turbulent heat transfer behind 2-D block

Figure 9 shows the distributions of C_f and St behind 2-D block. Also, the reattachment and maximum Stanton number

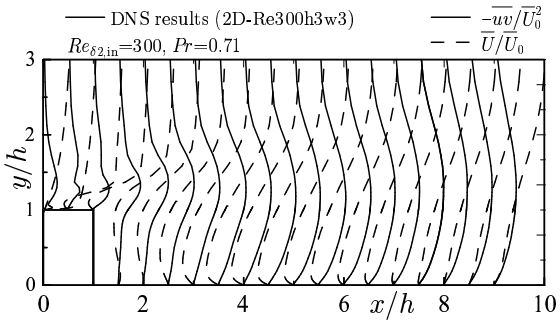

(a) Reynolds shear stresses and streamwise mean velocities

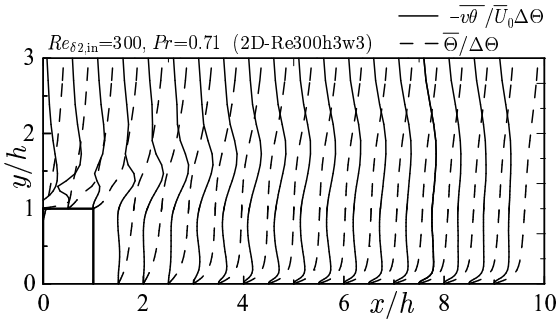

(b) Wall-normal turbulent heat fluxes and mean temperature

Figure 10. Distributions of turbulent quantities in boundary layer behind 2D-block (2D-Re300h3w3)

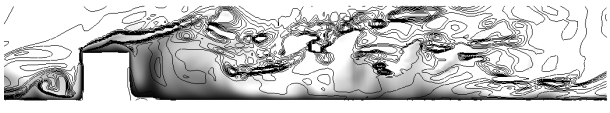

(a) $\omega_z < 0$

(b) $\omega_z > 0$

Figure 11. Distributions of instantaneous temperature and spanwise vorticity in boundary layer over 2D-block (2D-Re300h3w3)

points behind 2-D block are indicated in Tab. 1. As shown in Fig. 2, the recirculation region is formed behind 2-D block. The positive value of C_f near the 2-D block indicates the existing of secondary vortex in the recirculation region. The reattachment points, $X_r = (x-w)/h$, are located at $(x-w)/h \sim 8$ for cases of h3w3 and h6w6, and $(x-w)/h \sim 5$ for cases of h3w6 and h3w9. Because the flow reattaches on the block in cases of h3w6 and h3w9, the reattachment points of cases of h3w6 and h3w9 become shorter than that of cases of h3w3 and h6w6. Comparing with the experiment ($X_r = 6.7$) (Vogel and Eaton, 1985) and DNS ($X_r = 6.0$) (Le *et al.*, 1997) data of reattachment point in backward-facing step flow, all cases

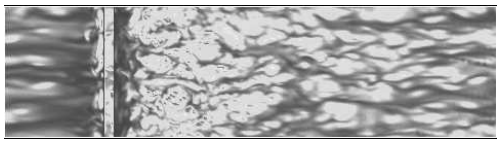

(a) Gradient of temperature, $\partial\theta/\partial y|_w$

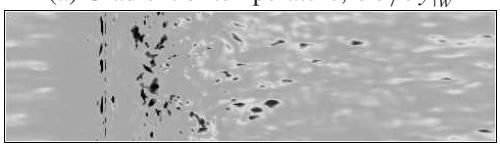

(b) Gradient of streamwise velocity, $\partial u/\partial y|_w$

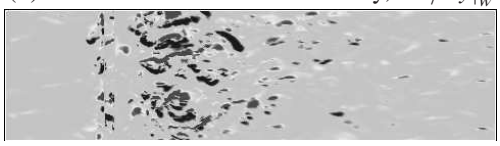

(c) Gradient of spanwise velocity, $\partial w/\partial y|_w$

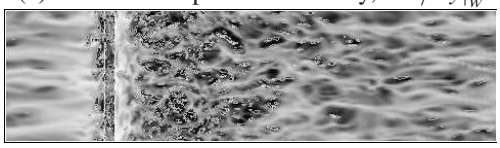

(d) Relation between $\partial\theta/\partial y|_w$ and near-wall vortex structure

Figure 12. Instantaneous turbulent quantities on vicinity of wall in boundary layer over 2D-block (2D-Re300h3w3)

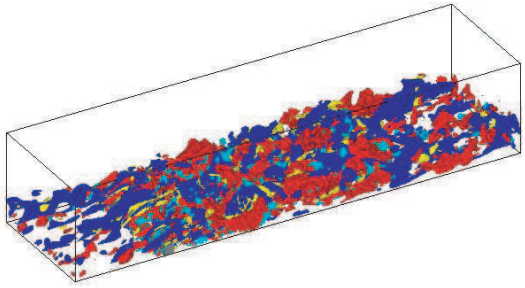

Figure 13. Quadrant analysis in 2-D block flow: $Q1$-event (sky blue), $Q2$-event (blue), $Q3$-event (yellow), and $Q4$-event (red)

do not agree with these data. The maximum Stanton number point is located shorter than the reattachment point except for case of 2D-Re300h3w6. This tendency agrees qualitatively with the experiment data Vogel and Eaton (1985).

Figure 10 shows distributions of Reynolds shear stress, streamwise mean velocity, wall-normal turbulent heat flux and mean temperature behind 2-D block in case of 2D-Re300h3w3. Although Reynolds shear stress increases in and above the recirculation region, the wall-normal turbulent heat flux has two peaks here, because the thermal boundary layer redevelops near the wall in the recirculation region. Thus, as for the distributions mean temperature, the double boundary layer of temperature can be seen, which was also observed in the experiment of turbulent boundary layer over 2-D hill (Houra *et al.*, 2007).

In order to investigate more detailed turbulent heat and mass transfer behind 2-D block, distributions of instantaneous

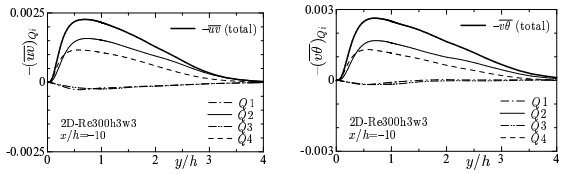

(a) $x/h = -10$

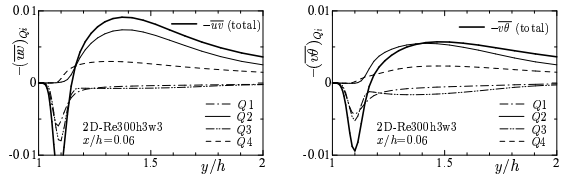

(b) $x/h = 0.06$

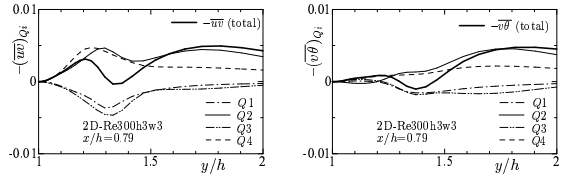

(c)$x/h = 0.79$

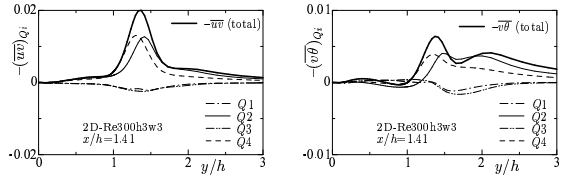

(d)$x/h = 1.41$

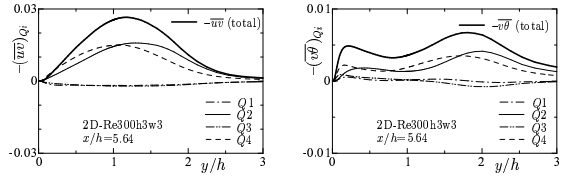

(e)$x/h = 5.64$

Figure 14. Quadrant analysis around 2-D block

temperature and spanwise vorticity, ω_z are shown in Fig. 11. Also, Fig. 12 shows instantaneous turbulent quantities on the vicinity of wall. It can be seen that the positive spanwise vortex contributes heat and mass transfer near the wall. However, it can be seen that the gradient of spanwise velocity, $\partial w/\partial y \sim \omega_x$, relates strongly the gradient of temperature rather than the gradient of streamwise velocity which relates ω_z from Figs. 12(a), (b) and (c).

Quadrant analysis of turbulent heat transfer in 2-D block flow

In order to investigate the turbulence motion for the production of Reynolds shear stress and wall-normal turbulent heat flux in the 2-D block flow, Figs. 13 and 14 show the result of quadrant analysis for Reynolds shear stress and wall-normal turbulent heat flux. In Fig. 13, the color contours indicate $Q1$(sky blue: interaction), $Q2$ (blue: ejection), $Q3$ (yellow: interaction), and $Q4$ (red: sweep), respectively. It can be observed that these events are enhanced in the separation region. In particular, $Q1$ and $Q3$ events often occur on the 2-D block due to appearance of the negative value of Reynolds shear stress as shown in Fig. 14(b). $Q1$ and $Q3$ events also affect obviously the negative value of wall-normal turbulent heat flux near here. Figures 14 can also reveal that the sweep event affects Reynolds shear stress and wall-normal turbulent heat flux near the wall at all locations except for near the wall behind the block.

CONCLUSIONS

DNSs of heat and mass transfer in turbulent boundary layers with separation and reattachment are carried out to investigate in detail the transport phenomena of such flows. The present DNS indicates the fundamental and detailed structures and mechanism of heat and mass transfer in turbulent boundary layers with separation and reattachment, in which the counter gradient phenomena of both the velocity and thermal fields are found on the step or block. Also, the quadrant analysis is carried out so as to investigate the turbulence motion for the production of Reynolds shear stress and wall-normal turbulent heat flux. It is revealed that $Q1$ and $Q3$ events (interactions) affect these quantities on the 2-D block.

ACKNOWLEDGMENT

This research was supported by a Grant-in-Aid for Scientific Research (C), 23560225, from the Japan Society for the Promotion of Science (JSPS).

REFERENCES

H. Hattori, T. Houra, and Y. Nagano. Direct numerical simulation of stable and unstable turbulent thermal boundary layers. *International Journal of Heat and Fluid Flow*, 28: 1262–1271, 2007.

H. Hattori and Y. Nagano. Investigation of turbulent boundary layer over forward-facing step via direct numerical simulation. *International Journal of Heat and Fluid Flow*, 31: 284–294, 2010.

H. Hattori, N. Ohiwa, M. Kozuka, and Y. Nagano. Improvement of nonlinear eddy diffusivity model for rotational turbulent heat transfer at various rotating axes. *Fluid Dynamics Research*, 41:012402 (26pages), 2009.

T. Houra, M. Tagawa, and Y. Nagano. Turbulence measurements of flows over a heated two-dimensional hill. *Proceedings of 2007 ASME-JSME Thermal Engineering Summer Heat Transfer Conference*, 18, Issue 1, February 1997: 6 pages in CD–ROM, 2007.

H. Le, P. Moin, and J. Kim. Direct numerical simulation of turbulent flow over a backward-facing step. *Journal of Fluid Mechanics*, 330:349–374, 1997.

J. C. Vogel and J. K. Eaton. Combined heat transfer and fluid dynamic measurements downstream of a backward-facing step. *Transaction of ASME, Journal of Heat Transfer*, 107: 922–929, 1985.